Contents

Part VI

PLASMA PHYSICS

Plasma Physics

Version 1019.1.K.pdf, April 1, 2009.

A *plasma* is a gas that is significantly ionized (through heating or photoionization) and thus is composed of electrons and ions, and that has a low enough density to behave classically, i.e. to obey Maxwell-Boltzmann statistics rather than Fermi-Dirac or Bose-Einstein. Plasma physics originated in the nineteenth century, in the study of gas discharges (Crookes 1879). However, it was soon realised that plasma is also the key to understanding the propagation of radio waves across the Atlantic (Heaviside 1902). The subject received a further boost in the early 1950s, with the start of the controlled (and the uncontrolled) thermonuclear fusion program. The various confinement devices described in the preceding chapter are intended to hold plasma at temperatures as high as $\sim 10^8$ K; the difficulty of this task has turned out to be an issue of plasma physics as much as MHD. After fusion, the next new venue for plasma research was extraterrestrial. Although it was already understood that the Earth was immersed in a tenuous outflow of ionized hydrogen known as the *solar wind*, the dawn of the space age in 1957 also initiated experimental *space plasma physics*. More recently, the interstellar and intergalactic media beyond the solar system as well as exotic astronomical objects like quasars and pulsars have allowed us to observe plasmas under quite extreme conditions, unreproducible in any laboratory experiment.

The dynamical behavior of a plasma is more complex than the dynamics of the gases and fluids we have met so far. This dynamical complexity has two main origins:

(i) The dominant form of interparticle interaction in a plasma, Coulomb scattering, is so weak that the mean free paths of the electrons and ions are often larger than the plasma's macroscopic length scales. This allows the particles' momentum distribution functions to deviate seriously from their equilibrium Maxwellian forms and, in particular, to be highly anisotropic.

(ii) The electromagnetic fields in a plasma are of long range. This allows charged particles to couple to each other electromagnetically and act in concert as modes of excitation (plasma waves or plasmons) that behave like single dynamical entities. Much of plasma physics consists of the study of the properties and interactions of these modes.

The dynamical behavior of a plasma depends markedly on frequency. At the lowest of frequencies the ions and electrons are locked together by electrostatic forces and behave like an electrically conducting fluid; this is the regime of magnetohydrodynamics (MHD; Chap. 17). At somewhat higher frequencies the electrons and the ions can move relative to

each other, behaving like two separate, interpenetrating fluids; we shall study this two-fluid regime in Chap. 19. At still higher frequencies, complex dynamics is supported by momentum space anisotropies and can be analyzed using a variant of the kinetic-theory collisionless Boltzmann equation that we introduced in Chap. 2. We shall study such dynamics in Chap. 20. In the two-fluid and collisionless-Boltzmann analyses of Chaps. 19 and 20 we focus on phenomena that can be treated as linear perturbations of an equilibrium state. However, the complexities and long mean free paths of plasmas also produce rich nonlinear phenomena; we shall study some of these in Chap. 21. As a foundation for the dynamical studies in Chaps. 19, 20, and 21, we develop in Chap. 18 detailed insights into the microscopic structure of a plasma.

Chapter 19

The Particle Kinetics of Plasma

Version 1019.1.K.pdf, April 1, 2009.
Please send comments, suggestions, and errata via email to kip@caltech.edu or on paper to Kip Thorne, 350-17 Caltech, Pasadena CA 91125

Box 19.1
Reader's Guide

- This chapter relies significantly on portions of nonrelativistic kinetic theory as developed in Chap. 2.
- It also relies a bit but not greatly on portions of magnetohydrodynamics as developed in Chap. 18.
- The remaining chapters 19-21 of Part V, Plasma Physics rely heavily on this chapter.

19.1 Overview

The preceding chapter, Chap. 17, can be regarded as a transition from fluid mechanics toward plasma physics: It described equilibrium and low-frequency dynamical phenomena in a magnetized plasma using fluid-mechanics techniques. In this chapter, we prepare for more sophisticated descriptions of plasma by introducing a number of elementary foundational concepts peculiar to plasma, and by exploring a plasma's structure on the scale of individual particles using elementary techniques from kinetic theory.

Specifically, in Sec. 19.2 we identify the region of densities and temperatures in which matter, in statistical equilibrium, takes the form of a plasma, and we meet a number of specific examples of plasmas that occur in Nature and in the laboratory. Then in Sec. 19.3 we study two phenomena that are important for plasmas: the collective manner in which

large numbers of electrons and ions shield out the electric field of a charge in a plasma (Debye shielding), and oscillations of a plasma's electrons relative to its ions (plasma oscillations).

In Sec. 19.4, we study the Coulomb scattering by which a plasma's electrons and ions deflect an individual charged particle from straight-line motion and exchange energy with it. We then examine the statistical properties of large numbers of such Coulomb scatterings—most importantly, the rates (inverse timescales) for the velocities of a plasma's electrons and ions to isotropise, and the rates for them to thermalize. Our calculations reveal that Coulomb scattering is so weak that, in most plasmas encountered in Nature, it is unlikely to produce isotropised or thermalized velocity distributions. In Sec. 19.5 we give a brief preview of the fact that in real plasmas the scattering of electrons and ions off collective plasma excitations (*plasmons*) will often isotropize and thermalize their velocities far faster than would Coulomb scattering, and will cause many real plasmas to be far more isotropic and thermalized than our Coulomb-scattering analyses suggest. We shall explore this "anomalous" behavior in Chaps. 21 and 22. Finally, in Sec. 19.5 use the statistical properties of Coulomb scatterings to derive a plasma's transport coefficients, specifically its electrical and thermal conductivities, for situations where Coulomb scattering dominates over particle-plasmon scattering.

Most plasmas are significantly magnetized. This introduces important new features into their dynamics which we describe in Sec. 19.6: cyclotron motion (the spiraling of particles around magnetic field lines), a resulting anisotropy of the plasma's pressure (different pressure along and orthogonal to the field lines), and the split of a plasma's adiabatic index into four different adiabatic indices for four different types of compression. Finally, in Sec. 19.7, we examine the motion of an individual charged particle in a slightly inhomogeneous and slowly time varying magnetic field, and we describe *adiabatic invariants* which control that motion in easily understood ways.

19.2 Examples of Plasmas and their Density-Temperature Regimes

The density-temperature regime in which matter behaves as a nonrelativistic plasma is shown in Fig. 19.1. In this figure, and in most of Part V, we shall confine our attention to pure hydrogen plasma comprising protons and electrons. Many plasmas contain large fractions of other ions, which can have larger charges and do have greater masses than protons. This generalization introduces few new issues of principle so, for simplicity, we shall eschew it.

The boundaries of the plasma regime in Fig. 19.1 are dictated by the following considerations:

19.2.1 Ionization boundary

We shall be mostly concerned with *fully* ionized plasmas, even though partially ionized plasmas such as the ionosphere are often encountered in physics, astronomy, and engineering. The plasma regime's ionization boundary is the bottom curve in Fig. 19.1, at a temperature of a few thousand degrees. This boundary is dictated by chemical equilibrium for the reaction

$$\mathrm{H} \leftrightarrow \mathrm{p} + \mathrm{e} \tag{19.1}$$

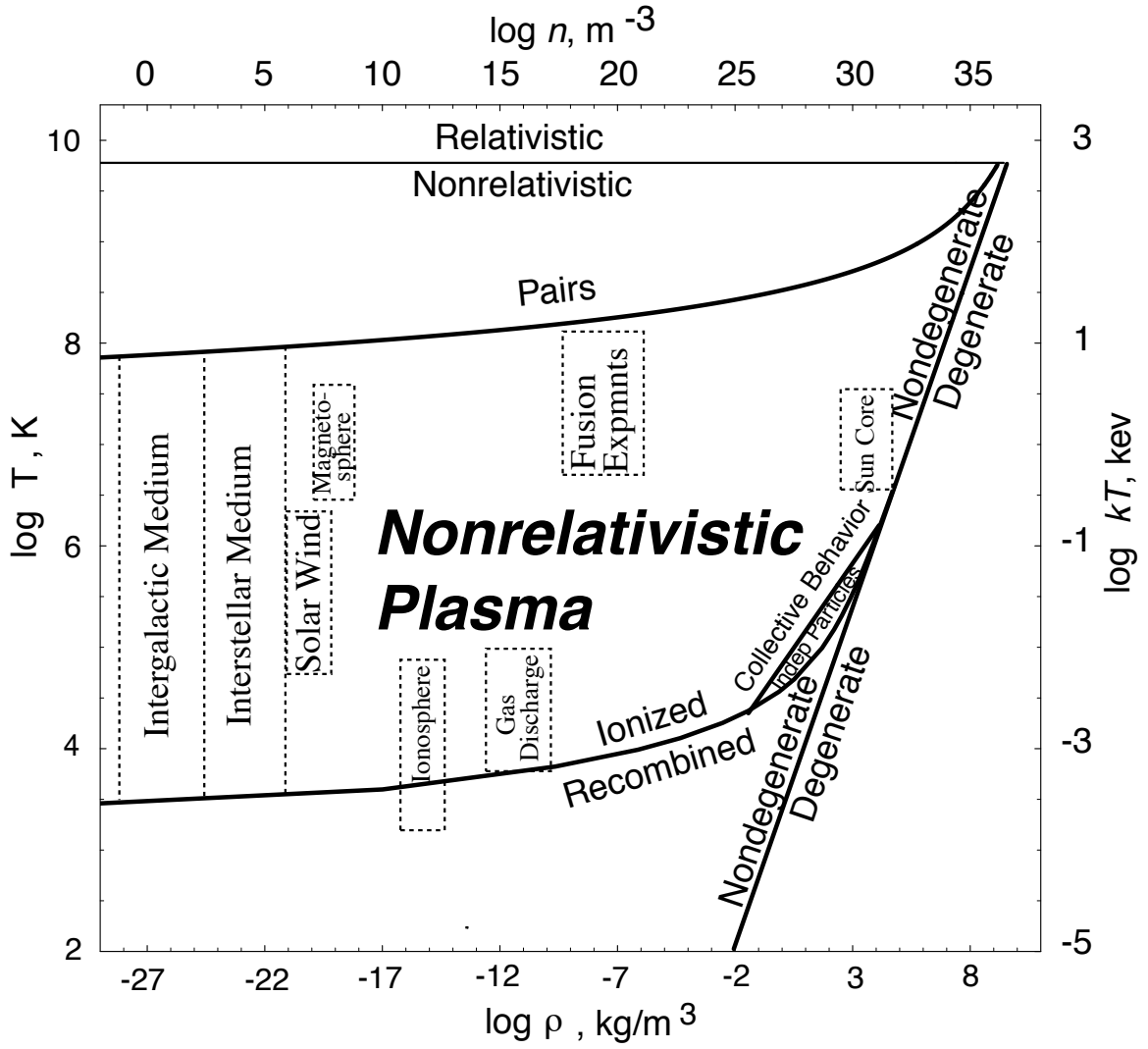

Fig. 19.1: The density-temperature regime in which matter, made largely of hydrogen, behaves as a nonrelativistic plasma. The densities and temperatures of specific examples of plasmas are indicated by dashed lines. The number density of electrons n is shown horizontally at the top, and the corresponding mass density ρ is shown at the bottom. The temperature T is shown at the left in degrees Kelvin, and at the right k_BT is shown in keV, thousands of electron volts.

as described by the Saha equation (Ex. 4.6):

$$\frac{n_e n_p}{n_H} = \frac{(2\pi m_e k_B T)^{3/2}}{h^3} e^{-I_P/k_B T} \ . \tag{19.2}$$

Here n_e, n_p, n_H are the number densities of electrons, protons, and neutral Hydrogen atoms (at the relevant temperatures hydrogen molecules have dissociated into individual atoms); T is temperature; m_e is the electron rest mass; h is Planck's constant; k_B is Boltzmann's constant; and $I_P = 13.6\,\mathrm{eV}$ is the ionization potential of hydrogen—i.e., the binding energy of its ground state. The boundary plotted in Fig. 19.1 is that of 50 percent ionization, i.e., $n_e = n_p = n_H = \rho/2m_H$ (with m_H the mass of a hydrogen atom); but because of the exponential factor in Eq. (19.2), the line of 90 percent ionization is virtually indistinguishable from that of 50 percent ionization on the scale of the figure. Using the rough equivalence $1\ \mathrm{eV} \cong 10^4\ \mathrm{K}$, we might have expected that the ionization boundary would correspond to a temperature $T \sim I_P/k_B \sim 10^5\ \mathrm{K}$. However this is true only near the degeneracy boundary (see below). When the plasma is strongly non-degenerate, ionization occurs at a significantly lower temperature due to the vastly greater number of states available to an electron when free than when bound in a hydrogen atom. Equivalently, at low densities, once a Hydrogen atom has been broken up into an electron plus a proton, the electron (or proton) must travel a large distance before encountering another proton (or electron) with which to recombine, making a new Hydrogen atom; as a result equilibrium occurs at a lowered temperature, where the ionization rate is thereby lowered to match the smaller recombination rate.

19.2.2 Degeneracy boundary

The electrons, with their small rest masses, become *degenerate* more easily than the protons or hydrogen atoms. The slanting line on the right side of Fig. 19.1 is the plasma's boundary of electron degeneracy. This boundary is determined by the demand that the mean occupation number of the electrons' single-particle quantum states not be $\ll 1$. In other words, the volume of phase space per electron, i.e. the product of the volumes of real space $\sim n_e^{-1}$ and of momentum space $\sim (m_e k_B T)^{3/2}$ occupied by each electron, should be comparable with the elementary quantum mechanical phase-space volume given by the uncertainty principle, h^3. Inserting the appropriate factors of order unity [cf. Eq. (2.39)], this relation becomes the boundary equation

$$n_e \simeq 2\frac{(2\pi m_e k_B T)^{3/2}}{h^3} \ . \tag{19.3}$$

When the electrons becomes degenerate (rightward of the degeneracy line in Fig. 19.1), as they do in a metal or a white dwarf star, the electron de Broglie wavelength becomes large compared with the mean interparticle spacing, and quantum mechanical considerations are of paramount importance.

19.2.3 Relativistic boundary

Another important limit arises when the electron thermal speeds become relativistic. This occurs when

$$T \sim m_e c^2/k_B \sim 6 \times 10^9\,\mathrm{K} \tag{19.4}$$

(top horizontal line in Fig. 19.1). Although we shall not consider them much further, the properties of relativistic plasmas (above this line) are mostly analogous to those of non-relativistic plasmas (below this line).

19.2.4 Pair-production boundary

Finally, for plasmas in statistical equilibrium, electron-positron pairs are created in profusion at high enough temperatures. In Ex. 4.5 we showed that, for $k_B T \ll m_e c^2$ but T high enough that pairs begin to form, the density of positrons divided by that of protons is

$$\frac{n_+}{n_p} = \frac{1}{2y[y + (1+y^2)^{1/2}]} \ , \quad \text{where } y \equiv \frac{1}{4} n_e \left(\frac{h}{\sqrt{2\pi m_e k_B T}} \right)^3 e^{m_e c^2/k_B T} \ . \tag{19.5}$$

Setting this expression to unity gives the pair-production boundary. This boundary curve, labeled "Pairs" in Fig. 19.1, is similar in shape to the ionization boundary but shifted in temperature by $\sim 2 \times 10^4 \sim \alpha_F^{-2}$, where α_F is the fine structure constant. This is because we are now effectively "ionizing the vacuum" rather than a hydrogen atom, and the "ionization potential of the vacuum" is $\sim 2 m_e c^2 = 4 I_P / \alpha_F^2$.

We shall encounter a plasma above the pair-production boundary, and thus with a profusion of electron-positron pairs, in our discussion of the early universe in Chap. 25.

19.2.5 Examples of natural and man-made plasmas

Figure 19.1 and Table 19.1 show the temperature-density regions for the following plasmas:

- *Laboratory gas discharge.* The plasmas created in the laboratory by electric currents flowing through hot gas, e.g., in vacuum tubes, spark gaps, welding arcs, and neon and fluorescent lights.
- *Controlled thermonuclear fusion experiments.* The plasmas in which experiments for controlled thermonuclear fusion are carried out, e.g., in tokamaks.
- *Ionosphere.* The part of the earth's upper atmosphere (at heights of $\sim 50 - 300$ km) that is partially photoionized by solar ultraviolet radiation.
- *Magnetosphere.* The plasma of high-speed electrons and ions that are locked onto the earth's dipolar magnetic field and slide around on its field lines at several earth radii.
- *Sun's core.* The plasma at the center of the sun, where fusion of hydrogen to form helium generates the sun's heat.
- *Solar wind.* The wind of plasma that blows off the sun and outward through the region between the planets.
- *Interstellar medium.* The plasma, in our Galaxy, that fills the region between the stars; this plasma exhibits a fairly wide range of density and temperature as a result of such processes as heating by photons from stars, heating and compression by shock waves from supernovae, and cooling by thermal emission of radiation.

Plasma	n_e (m^{-3})	T (K)	B (T)	λ_D (m)	N_D	ω_p (s^{-1})	ν_{ee} (s^{-1})	ω_c (s^{-1})	r_L (m)
Gas discharge	10^{16}	10^4	—	10^{-4}	10^4	10^{10}	10^5	—	—
Tokamak	10^{20}	10^8	10	10^{-4}	10^8	10^{12}	10^4	10^{12}	10^{-5}
Ionosphere	10^{12}	10^3	10^{-5}	10^{-3}	10^5	10^8	10^3	10^6	10^{-1}
Magnetosphere	10^7	10^7	10^{-8}	10^2	10^{10}	10^5	10^{-8}	10^3	10^4
Solar core	10^{32}	10^7	—	10^{-11}	1	10^{18}	10^{16}	—	—
Solar wind	10^6	10^5	10^{-9}	10	10^{11}	10^5	10^{-6}	10^2	10^4
Interstellar medium	10^5	10^4	10^{-10}	10	10^{10}	10^4	10^{-5}	10	10^4
Intergalactic medium	1	10^6	—	10^5	10^{15}	10^2	10^{-13}	—	—

Table 19.1: Representative densities, temperatures and magnetic field strengths together with derived plasma parameters in a variety of environments. For definitions, see text. Values are given to order of magnitude as all of these environments are quite inhomogeneous.

- *Intergalactic medium.* The plasma that fills the space outside galaxies and clusters of galaxies; we shall meet the properties and evolution of this intergalactic plasma in our study of cosmology, in the last chapter of this book.

Characteristic plasma properties in these various environments are collected in Table 19.1. In the next three chapters we shall study applications from all these environments.

****

EXERCISES

Exercise 19.1 *Derivation: Boundary of Degeneracy*
Show that the condition $n_e \ll (m_e k_B T)^{3/2}/h^3$ [cf. Eq. (19.3)] that electrons be nondegenerate is equivalent to the following statements:

(a) The mean separation between electrons, $l \equiv n_e^{-1/3}$, is large compared to the de Broglie wavelength, $\lambda\!\!\!^{-}_{\rm dB} = \hbar/(\text{momentum})$, of an electron whose kinetic energy is $k_B T$.

(b) The uncertainty in the location of an electron drawn at random from the thermal distribution is small compared to the average inter-electron spacing.

(c) The quantum mechanical zero-point energy associated with squeezing each electron into a region of size $l = n_e^{-1/3}$ is small compared to the electron's mean thermal energy $k_B T$.

****

19.3 Collective Effects in Plasmas – Debye Shielding and Plasma Oscillations

In this section we introduce two key ideas that are associated with most of the collective effects in plasma dynamics: Debye shielding and plasma oscillation.

19.3.1 Debye Shielding

Any charged particle inside a plasma attracts other particles with opposite charge and repels those with the same charge, thereby creating a net cloud of opposite charges around itself. This cloud shields the particle's own charge from external view; i.e., it causes the particle's Coulomb field to fall off exponentially at large radii, rather than falling off as $1/r^2$. [1]

This Debye shielding of a particle's charge can be demonstrated and quantified as follows: Consider a single fixed test charge Q surrounded by a plasma of protons and electrons. Let us define average densities for electrons and protons as smooth functions of radius r from the test charge, $n_p(r), n_e(r)$ and let the mean densities of electrons and protons (which must be equal because there must be overall charge neutrality) be $\bar{n}$. Then the electrostatic potential $\Phi(r)$ outside the particle satisfies Poisson's equation, which we write in SI units:[2]

$$\nabla^2\Phi = -\frac{(n_p - n_e)e}{\epsilon_0} - \frac{Q}{\epsilon_0}\delta(\mathbf{r}) \ . \tag{19.6}$$

(We denote the positive charge of a proton by $+e$ and the negative charge of an electron by $-e$.)

A proton at radius r from the particle has an electrostatic potential energy $e\Phi(r)$. Correspondingly, the number density of protons at radius r is altered from $\bar{n}$ by the Boltzmann factor $\exp(-e\Phi/k_BT)$; and, similarly, the density of electrons is altered by $\exp(+e\Phi/k_BT)$:

$$\begin{aligned} n_p &= \bar{n}\exp(-e\Phi/k_BT) \simeq \bar{n}(1 - e\Phi/k_BT) \ , \\ n_e &= \bar{n}\exp(+e\Phi/k_BT) \simeq \bar{n}(1 + e\Phi/k_BT) \ . \end{aligned} \tag{19.7}$$

where we have made a Taylor expansion of the Boltzmann factor valid for $e\Phi \ll k_BT$. By inserting the linearized versions of Eq. (19.7) into (19.6), we obtain

$$\nabla^2\Phi = \frac{2e^2\bar{n}}{\epsilon_0 k_B T}\Phi - \frac{Q}{\epsilon_0}\delta(\mathbf{r}) \ . \tag{19.8}$$

The spherically symmetric solution to this equation,

$$\boxed{\Phi = \frac{Q}{4\pi\epsilon_0 r}e^{-\sqrt{2}r/\lambda_D} \ ,} \tag{19.9}$$

[1] Analogous effects are encounted in condensed matter physics and quantum electrodynamics.

[2] For those who prefer Gaussian units the translation is most easily effected by the transformations $4\pi\epsilon_0 \to 1$ and $\mu_0/4\pi \to 1$, and inserting factors of c by inspection using dimensional analysis. It is also useful to recall that 1 T$\equiv 10^4$ Gauss and that the charge on an electron is -1.6×10^{-19} C$\equiv -4.8\times10^{-10}$ esu.

has the form of a Coulomb field with an exponential cutoff. [3] The characteristic lengthscale of the exponential cutoff,

$$\boxed{\lambda_D \equiv \left(\frac{\epsilon_0 k_B T}{\bar{n} e^2}\right)^{1/2} = 69 \left(\frac{T/1\mathrm{K}}{\bar{n}/1\,\mathrm{m}^{-3}}\right)^{1/2} \mathrm{m},} \tag{19.10}$$

is called the *Debye length*. It is a rough measure of the size of the Debye shielding cloud that the charged particle carries with itself.

The charged particle could be some foreign charged object (not a plasma electron or proton), or equally well, it could be one of the plasma's own electrons or protons. Thus, we can think of each electron in the plasma as carrying with itself a positively charged Debye shielding cloud of size λ_D, and each proton as carrying a negatively charged cloud. Each electron and proton not only carries its own cloud; it also plays a role as one of the contributors to the clouds around other electrons and protons.

19.3.2 Collective behavior

A charged particle's Debye cloud is almost always made of a huge number of electrons, and very nearly the same number of protons. It is only a tiny, time-averaged excess of electrons over protons (or protons over electrons) that produces the cloud's net charge and the resulting exponential decay of the electrostatic potential. Ignoring this tiny excess, the mean number of electrons in the cloud and the mean number of protons are roughly

$$\boxed{N_{\mathrm{D}} \equiv \bar{n} \frac{4\pi}{3} {\lambda_D}^3 = 1.4 \times 10^6 \frac{(T/1\mathrm{K})^{3/2}}{(\bar{n}/1\,\mathrm{m}^{-3})^{1/2}}\ .} \tag{19.11}$$

This *Debye number* is large compared to unity throughout the density-temperature regime of plasmas, except for the tiny lower right-hand corner of Fig. 19.1. The boundary of that corner region (labeled "Collective behavior / Independent Particles") is given by $N_D = 1$. The upper left-hand side of that boundary has $N_D \gg 1$ and is called the "regime of collective behavior" because a huge number of particles are collectively responsible for the Debye cloud, and this leads to a variety of collective dynamical phenomena in the plasma. The lower right-hand side has $N_D < 1$ and is called the "regime of independent particles" because in it collective phenomena are of small importance. In this book we shall restrict ourselves to the huge regime of collective behavior and ignore the tiny regime of independent particles.

Characteristic values for the Debye length in a variety of environments are collected in Table 19.1.

19.3.3 Plasma Oscillations and Plasma Frequency

Of all the dynamical phenomena that can occur in a plasma, perhaps the most important is a relative oscillation of the plasma's electrons and protons. The simplest version of this *plasma oscillation* is depicted in Fig. 19.2. Suppose for the moment that the protons are all

[3] In nuclear physics this potential is known as a *Yukawa potential*.

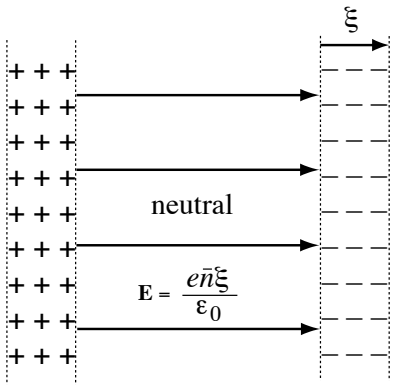

Fig. 19.2: Idealized depiction of the displacement of electrons relative to protons, which occurs during plasma oscillations.

fixed and displace the electrons rightward (in the x-direction) with respect to the protons by an amount ξ, thereby producing a net negative charge per unit area $-e\bar{n}\xi$ at the right end of the plasma, a net positive charge per unit area $+e\bar{n}\xi$ at the left end, and a corresponding electric field $E = e\bar{n}\xi/\epsilon_0$ in the x-direction throughout the plasma. The electric field pulls on the plasma's electrons and protons, giving the electrons an acceleration $d^2\xi/dt^2 = -eE/m_e$ and the protons an acceleration smaller by $m_e/m_p = 1/1860$, which we shall neglect. The result is an equation of motion for the electrons' collective displacement:

$$\frac{d^2\xi}{dt^2} = -\frac{e}{m_e}E = -\frac{e^2\bar{n}}{\epsilon_0 m_e}\xi \ . \tag{19.12}$$

Since Eq. (19.12) is a harmonic-oscillator equation, the electrons oscillate sinusoidally, $\xi = \xi_o \cos(\omega_p t)$, at the *plasma frequency*

$$\boxed{\omega_p \equiv \left(\frac{\bar{n}e^2}{\epsilon_0 m_e}\right)^{1/2} = 56.4 \left(\frac{\bar{n}}{1\,\mathrm{m}^{-3}}\right)^{1/2} \mathrm{s}^{-1} \ .} \tag{19.13}$$

Notice that this frequency of plasma oscillations depends only on the plasma density $\bar{n}$ and not on its temperature or on the strength of any magnetic field that might be present. Note that if we define the electron thermal speed to be $v_e \equiv (k_B T_e/m_e)^{1/2}$, then $\omega_p \equiv v_e/\lambda_D$. In other words a thermal electron travels about a Debye length in a plasma period. Just as the Debye length functions as the electrostatic correlation length, so the plasma period plays the role of the electrostatic correlation time.

Characteristic values for the plasma frequency in a variety of environments are collected in Table 19.1.

19.4 Coulomb Collisions

In this section we will study transport coefficients (electrical and thermal conductivities) and the establishment of local thermodynamic equilibrium in a plasma under the hypothesis

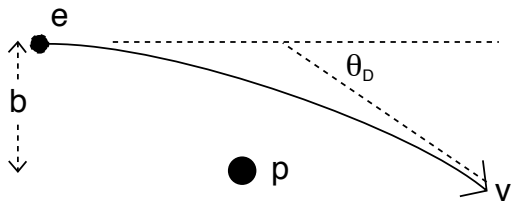

Fig. 19.3: The geometry of a Coulomb collision.

that Coulomb collisions provide the dominant source of scattering for both electrons and protons. In fact, as we shall see later, Coulomb scattering is usually a less effective scattering mechanism than *collisionless* processes mediated by fluctuating electromagnetic fields.

19.4.1 Collision frequency

Consider first, as we did in our discussion of Debye screening, a single test particle — let it be an electron — interacting with background field particles — let these be protons for the moment. The test electron moves with speed v_e. The field protons will move much more slowly if they are near thermodynamic equilibrium (as their masses are much greater than those of the electrons), so they can be treated, for the moment, as at rest. When the electron flies by a single proton, we can characterize the encounter using an *impact parameter* b, which is what the distance of closest approach would have been if the electron were not deflected; see Fig. 19.3. The electron will be scattered by the Coulomb field of the proton, a process sometimes called *Rutherford scattering*. If the deflection angle is small, $\theta_D \ll 1$, we can approximate its value by computing the perpendicular impulse exerted by the Coulomb field of the proton integrating along the unperturbed straight line trajectory.

$$m_e v_e \theta_D = \int_{-\infty}^{+\infty} \frac{e^2 b}{4\pi\epsilon_o (b^2 + v_e^2 t^2)^{3/2}} dt = \frac{e^2}{2\pi\epsilon_o v_e b} \ , \tag{19.14}$$

This implies that

$$\theta_D = b_o/b \text{ for } b \gg b_o \ , \tag{19.15}$$

where

$$b_o \equiv \frac{e^2}{2\pi\epsilon_0 m_e v_e^2} \ . \tag{19.16}$$

When $b \lesssim b_0$, this approximation breaks down and the deflection angle is of order a radian.[4]

Below we shall need to know how much energy the electron loses, for the large-impact-parameter case. That energy loss, $-\Delta E$, is equal to the energy gained by the proton. Since the proton is initially at rest, and since momentum conservation implies it gains a momentum $\Delta p = m_e v_e \theta_D$, ΔE must be

$$\Delta E = -\frac{(\Delta p)^2}{2m_p} = -\frac{m_e}{m_p}\left(\frac{b_o}{b}\right)^2 E \quad \text{for } b \gg b_o \ . \tag{19.17}$$

[4]A more careful calculation gives $2\tan\theta_D/2 = b_o/b$, see *e.g.* Leighton (1959).

Here $E = \frac{1}{2} m_e v_e^2$ is the electron's initial energy.

We turn, next, from an individual Coulomb collision to the net, statistically averaged effect of many collisions. The first thing we shall compute is the mean time t_D required for the orbit of the test electron to be deflected by an angle of order a radian from its initial direction, and the inverse of t_D: the "deflection rate" or "deflection frequency" $\nu_D = 1/t_D$. If the dominant source of this deflection were a single large-angle scattering event, then the relevant cross section would be $\sigma = \pi b_o^2$ (since all impact parameters $\lesssim b_o$ produce large-angle scatterings), and the mean deflection time and frequency would be

$$\nu_D \equiv \frac{1}{t_D} = n\sigma v_e = n\pi b_o^2 v_e \quad \text{(single large-angle scattering of an electron by a proton).} \tag{19.18}$$

Here n is the proton number density, which is the same as the electron number density in our hydrogen plasma.

The cumulative, random-walk effects of many small-angle scatterings off field protons actually produce a net deflection of order a radian in a time shorter than this. As the directions of the individual scatterings are random, the mean deflection angle after many scatterings vanishes. However, the mean square deflection angle, $\langle \Theta^2 \rangle = \sum_{\text{all encounters}} \theta_D^2$ will not vanish. That mean square deflection angle, during a time t, accumulates up to

$$\langle \Theta^2 \rangle = \int_{b_{\min}}^{b_{\max}} \left(\frac{b_o}{b}\right)^2 n v_e t 2\pi b db = n 2\pi b_o^2 v_e t \, \ln\left(\frac{b_{\max}}{b_{\min}}\right) \ . \tag{19.19}$$

Here the factor $(b_o/b)^2$ in the integrand is the squared deflection angle θ_D^2 for impact parameter b, and the remaining factor $n v_e t 2\pi b db$ is the number of encounters that occur with impact parameters between b and $b + db$ during time t. The integral diverges logarithmically at both its lower limit $b_{\min}$ and its upper limit $b_{\max}$. Below we shall discuss the physical origins of and values of the cutoffs $b_{\min}$ and $b_{\max}$. The value of t that makes the mean square deflection angle $\langle \Theta^2 \rangle$ equal to unity is, to within factors of order unity, the deflection time t_D (and inverse deflection frequency ν_D^{-1}):

$$\boxed{\nu_D^{ep} = \frac{1}{t_D^{ep}} = n 2\pi b_o^2 v_e \, \ln\Lambda \ = \frac{n e^4 \ln\Lambda}{2\pi \epsilon_0^2 m_e^2 v_e^3} \ , \quad \text{where } \Lambda = b_{\max}/b_{\min} \ .} \tag{19.20}$$

Here the superscript ep indicates that the test particle is an electron and the field particles are protons. Notice that this deflection frequency is larger, by a factor $2\ln\Lambda$, than the frequency (19.18) for a single large-angle scattering.

We must also consider the repulsive collisions of our test electron with field electrons. Although we are no longer justified in treating the field electrons as being at rest, the impact parameter for a large angle deflection is still $\sim b_0$, so Eq. (19.20) is also appropriate to this case, in order of magnitude:

$$\boxed{\nu_D^{ee} = \frac{1}{t_D^{ee}} \sim \nu_D^{ep} \sim n 2\pi b_o^2 v_e \, \ln\Lambda \ = \frac{n e^4 \ln\Lambda}{2\pi \epsilon_0^2 m_e^2 v_e^3} \ .} \tag{19.21}$$

Finally, and in the same spirit, we can compute the collision frequency for the protons. Because electrons are so much lighter than protons, proton-proton collisions will be more effective in deflecting protons than proton-electron collisions. Therefore, the proton collision frequency is given by Eqs. (19.21) with the electron subscripts replaced by proton subscripts

$$\boxed{\nu_D^{pp} = \frac{1}{t_D^{pp}} \sim \frac{ne^4 \ln\Lambda}{2\pi\epsilon_0^2 m_p^2 v_p^3} \ .} \tag{19.22}$$

19.4.2 The Coulomb logarithm

The maximum impact parameter $b_{\max}$, which appears in $\Lambda \equiv b_{\max}/b_{\min}$, is the Debye length λ_D, since at impact parameters $b \gg \lambda_D$ the Debye shielding screens out the field particle's Coulomb field, while at $b \ll \lambda_D$ Debye shielding is unimportant.

The minimum impact parameter $b_{\min}$ has different values depending on whether quantum mechanical wave packet spreading is important or not for the test particle during the collision. Because of wave-function spreading, the nearest the test particle can come to a field particle is the test particle's de Broglie wavelength, i.e., $b_{\min} = \hbar/mv$. However if the de Broglie wavelength is smaller than b_0, then the effective value of $b_{\min}$ will be simply b_0. In summary,

$$\begin{aligned} b_{\min} &= \max[b_o = 2e^2/m_e v_e^2 \ , \ \hbar/m_e v_e] \ , \quad \text{and } b_{\max} = \lambda_D \quad \text{for test electrons ;} \\ b_{\min} &= \max[b_o = 2e^2/m_p v_p^2 \ , \ \hbar/m_p v_p] \ , \quad \text{and } b_{\max} = \lambda_D \quad \text{for test protons .} \end{aligned} \tag{19.23}$$

Over most of the accessible range of density and temperature for a plasma, $3 \lesssim \ln\Lambda \lesssim 30$. Therefore if we set

$$\boxed{\ln\Lambda \simeq 10 \ ,} \tag{19.24}$$

our estimate is good to a factor ~ 3. For tables of $\ln\Lambda$, see Spitzer (1962).

19.4.3 Thermal Equilibration Times in a Plasma

Suppose that a hydrogen plasma is heated in some violent way (e.g., by a shock wave). Such heating will typically give the plasma's electrons and protons a non-Maxwellian velocity distribution. Coulomb collisions will then, as time passes, (and in the absence of more violent disruptions), force the particles to exchange energy in random ways, and will gradually drive them into thermal equilibrium. This thermal equilibration is achieved at different rates for the electrons and the protons, and correspondingly the following three timescales are all different:

$$\begin{aligned} t_{ee}^{\rm eq} &\equiv \left(\begin{array}{c} \text{time required for electrons to equilibrate with each other,} \\ \text{achieving a near Maxwellian velocity distribution} \end{array} \right) \ , \\ t_{pp}^{\rm eq} &\equiv (\text{time for protons to equilibrate with each other}) \ , \\ t_{ep}^{\rm eq} &\equiv (\text{time for electrons to equilibrate with protons}) \ . \end{aligned} \tag{19.25}$$

In this section we shall compute these three equilibration times.

Electron-electron equilibration. In evaluating $t_{ee}^{\rm eq}$, we shall assume that the electrons begin with typical individual energies of order $k_B T_e$, where T_e is the temperature to which they are

going to equilibrate, but their initial velocity distribution is rather non-Maxwellian. Then we can choose a typical electron as the "test particle". We have argued that Coulomb interactions with electrons and protons are comparably effective in *deflecting* test electrons. However, they are not comparably effective in transferring energy. When the electron collides with a stationary proton, the energy transfer is

$$\frac{\Delta E}{E} \simeq -\frac{m_e}{m_p}\theta_D^2 \tag{19.26}$$

[Eq. (19.17)]. This is smaller than the typical energy transfer in an electron-electron collision by the ratio m_e/m_p. Therefore it is the collisions between the electrons that are responsible for establishing an electron Maxwellian distribution function.

The alert reader may spot a problem at this point. According to Eq. (19.26), electrons always lose energy to protons and never gain it. This would cause the electron temperature to continue to fall below the proton temperature, in clear violation of the second law of thermodynamics. Actually what happens in practice is that if we allow for the finite proton velocities, then the electrons can gain energy from some electron-proton collisions. This is also the case for the electron-electron collisions of immediate concern. The correct formalism for dealing with this situation is the *Fokker-Planck formalism*, discussed in Sec. 5.7. Fokker-Planck is appropriate because, as we have shown, many weak scatterings dominate the few strong scatterings. If we use the Fokker-Planck approach to define an energy equilibration time for a nearly Maxwellian distribution of electrons with temperature T, then it turns out that a simple estimate based on combining the deflection time, given by Eq. (19.18) with the typical energy transfer estimated in relation (19.26) and assuming a typical velocity $v = (3k_BT/m_e)^{1/2}$ gives an answer good to a factor 2. It is actually convenient to express the energy equilibration timescale using its reciprocal, the *electron-electron equilibration rate*, ν_{ee}. This facilitates comparison with the other frequencies characterizing the plasma. The true Fokker-Planck estimate for electrons near equilibrium is then

$$\boxed{\nu_{ee} = \frac{n\sigma_T c \ln\Lambda}{2\pi^{1/2}}\left(\frac{k_BT_e}{m_ec^2}\right)^{-3/2} = 2.5\times10^{-5}\left(\frac{n}{1\mathrm{m}^{-3}}\right)\left(\frac{T_e}{1\mathrm{K}}\right)^{-3/2}\left(\frac{\ln\Lambda}{10}\right)\ \mathrm{s}^{-1},} \tag{19.27}$$

where we have used the Thomson cross section

$$\sigma_T = (8\pi/3)(e^2/4\pi\epsilon_0 m_e c^2)^2 = 6.65\times10^{-29}\ \mathrm{m}^2\ . \tag{19.28}$$

As for proton deflections [Eq. (19.22)], so also for proton energy equilibration, the light electrons are far less effective at influencing the protons than are other protons. Therefore, the protons achieve a thermal distribution by equilibrating with each other, and their *proton-proton equilibration rate* can be written down immediately from Eq. (19.27) by replacing the electron masses and temperatures with the protonic values.

$$\boxed{\nu_{pp} = \frac{n\sigma_T c \ln\Lambda}{2\pi^{1/2}}\left(\frac{m_e}{m_p}\right)^{1/2}\left(\frac{k_BT_p}{m_ec^2}\right)^{-3/2} = 5.8\times10^{-7}\left(\frac{n}{1\mathrm{m}^{-3}}\right)\left(\frac{T_p}{1\mathrm{K}}\right)^{-3/2}\left(\frac{\ln\Lambda}{10}\right)\ \mathrm{s}^{-1}.} \tag{19.29}$$

Finally, if the electrons and protons have different temperatures, we should compute the timescale for the two species to equilibrate with each other. This again is easy to estimate using the energy transfer equation (19.26): $t_{ep} \simeq (m_p/m_e)t_{ee}$ The more accurate Fokker-Planck result for the *electron-proton equilibration rate* is again very close and is given by

$$\boxed{\nu_{ep} = \frac{2n\sigma_T c \ln\Lambda}{\pi^{1/2}} \left(\frac{m_e}{m_p}\right) \left(\frac{k_B T_e}{m_e c^2}\right)^{-3/2} = 4.0 \times 10^{-8} \left(\frac{n}{1\mathrm{m}^{-3}}\right) \left(\frac{T_e}{1\mathrm{K}}\right)^{-3/2} \left(\frac{\ln\Lambda}{10}\right) \ \mathrm{s}^{-1}.} \tag{19.30}$$

Thus, *at the same density and temperature, protons require* $\sim (m_p/m_e)^{1/2} = 43$ *times longer to reach thermal equilibrium among themselves than do the electrons, and proton-electron equilibration takes a time* $\sim (m_p/m_e) = 1836$ *longer than electron-electron equilibration.*

19.4.4 Discussion

In Table 19.1, we show the electron-electron equilibration rates for a variety of plasma environments. Generically, they are very small compared with the plasma frequencies. For example, if we take parameters appropriate to a Tokamak, we find that $\nu_{ee} \sim 10^{-8}\omega_p$ and $\nu_{ep} \sim 10^{-11}\omega_p$. In fact we can see that the equilibration time is comparable, to order of magnitude, with the total plasma confinement time ~ 0.1 s (cf. section 17.3) . The disparity between ν_e and ω_p is even greater in the interstellar medium. For this reason most plasmas are well described as collisionless and we must anticipate that the particle distribution functions will depart significantly from Maxwellian form.

****

EXERCISES

Exercise 19.2 *Derivation: Coulomb logarithm*

(a) Express the Coulomb logarithm in terms of the Debye number, N_D, in the classical regime, when $b_{\min} \sim b_0$.

(b) Use the representative parameters from Table 19.1 to evaluate Coulomb logarithms for the sun's core, a Tokamak, and the interstellar medium, and verify that they lie in the range $3 \lesssim \ln\Lambda \lesssim 30$.

Exercise 19.3 *Derivation: Electron-electron collision rate*
Using the non-Fokker-Planck arguments outlined in the text, compute an estimate of the electron-electron equilibration rate and show that it agrees with the Fokker-Planck result, Eq. (19.27), to within a factor 2.

Exercise 19.4 *Problem: Dependence of thermal equilibration on charge and mass*
Compute the ion equilibration rate for a pure He^3 plasma with electron density 10^{20} m^{-3} and temperature 10^8 K.

Exercise 19.5 *Example: Stopping of α-particles*
A 100 MeV α-particle is incident upon a plastic containing electrons with density $n_e = 2 \times 10^{29}$ m^{-3}. Estimate the distance that it will travel before coming to rest. This is known as the *range*. (Ignore relativistic corrections and refinements such as the *density effect*. However, do consider the appropriate values of $b_{\max}$, $b_{\min}$.)

Exercise 19.6 *Example: Parameters for Various Plasmas*
Estimate the Debye length λ_D, the Debye number N_D, the plasma frequency $f_p \equiv \omega_p/2\pi$ and the electron deflection timescale $t_D^{ee} \sim t_D^{ep}$, for the following plasmas.

(a) An atomic bomb explosion in the Earth's atmosphere one millisecond after the explosion. [Use the Sedov-Taylor similarity solution for conditions behind the bomb's shock wave; Sec. 16.6.]

(b) The ionized gas that envelopes the Space Shuttle [cf. Box 16.2] as it re-enters the Earth's atmosphere.

(c) The expanding universe during its early evolution, just before it became cool enough for electrons and protons to combine to form neutral hydrogen (i.e., just before ionization "turned off"). [As we shall discover in Chap. 25, the universe today is filled with black body radiation, produced in the big bang, that has a temperature $T = 2.7\,\mathrm{K}$, and the universe today has a mean density of hydrogen $\rho \sim 1 \times 10^{-29}\,\mathrm{g/cm^3}$. Extrapolate backward in time to infer the density and temperature at the epoch just before ionization turned off.]

Exercise 19.7 *Problem: Equilibration Time for a Globular Star Cluster*
Stars have many similarities to electrons and ions in a plasma. These similarities arise from the fact that in both cases the interaction between the individual particles (stars, or ions and electrons) is a radial, $1/r^2$ force. The principal difference is the fact that the force between stars is always attractive, so there is no analog of Debye shielding. One consequence of this difference is the fact that a plasma can be spatially homogeneous and static, when one averages over length scales large compared to the interparticle separation; but a collection of stars cannot be: The stars congregate into clusters that are held together by the stars' mutual gravity.
A globular star cluster is an example. A typical globular cluster is a nearly spherical swarm of stars with the following parameters: (cluster radius)$\equiv R = 10$ light years; (total number of stars in the cluster) $\equiv N = 10^6$; and (mass of a typical star)$\equiv m =$ (0.4 solar masses)$= 8 \times 10^{32}$ grams. Each star moves on an orbit of the average, "smeared out" gravitational field of the entire cluster; and since that smeared-out gravitational field is independent of time, each star conserves its total energy (kinetic plus gravitational) as it moves. Actually, the total energy is only approximately conserved. Just as in a plasma, so also here, gravitational "Coulomb collisions" of the star with other stars produce changes of the star's energy.

(a) What is the mean time t_E for a typical star to change its energy substantially? Express your answer, accurate to within a factor ~ 3, in terms of N, R, and m; evaluate it numerically and compare it with the age of the Universe.

(b) The cluster evolves substantially on the timescale t_E. What type of evolution would you expect to occur? What type of stellar energy distribution would you expect to result from this evolution? [5]

****

19.5 Transport Coefficients

Because electrons have far lower masses than ions, they have far higher typical speeds at fixed temperature and are much more easily accelerated; i.e., they are much more mobile. As a result, it is the motion of the electrons, not the ions, that is responsible for the transport of heat and charge through a plasma. In the spirit of the discussion above, we can now compute transport properties such as the electric conductivity and thermal conductivity on the presumption that it is Coulomb collisions that determine the electron mean free paths and that magnetic fields are unimportant. (Later we will see that collisionless effects usually provide a more serious impediment to charge and heat flow than Coulomb collisions and thus dominate the conductivities.)

Consider, first, an electron exposed to a constant, accelerating electric field E. The electron's typical drift velocity along the direction of the electric field is $-eE/m_e\nu_D$, where ν_D is the deflection frequency (rate) evaluated in Eqs. (19.20) and (19.21). The associated current density is therefore $j \sim ne^2E/m_e\nu_D$, and the electrical conductivity is $\kappa_e \sim ne^2/m_e\nu_D$. (Note that electron-electron collisions conserve momentum and do not impede the flow of current, so electron-proton collisions, which happen about as frequently, produce all the electrical resistance and are thus responsible for this κ_e.)

The thermal conductivity can likewise be estimated by noting that a typical electron travels a mean free path $\ell \sim v_e/\nu_D$ from a location where the average temperature is different by an amount $\Delta T \sim \ell|\nabla T|$. The heat flux transported by the electrons is therefore $\sim nv_ek\Delta T$ which should be equated to $-\kappa\nabla T$. We therefore obtain the electron contribution to the thermal conductivity as $\kappa \sim nk_B^2T/m_e\nu_D$.

Computations based on the Fokker-Planck approach[6] produce equations for the electrical and thermal conductivities that agree with the above estimates to within factors of order unity:

$$\boxed{\kappa_e = 4.9\left(\frac{e^2}{\sigma_T c\ln\Lambda m_e}\right)\left(\frac{k_BT_e}{m_ec^2}\right)^{3/2} = 1.5\times10^{-3}\left(\frac{T_e}{1\mathrm{K}}\right)^{3/2}\left(\frac{\ln\Lambda}{10}\right)^{-1}\ \Omega^{-1}\mathrm{m}^{-1}\ ,} \quad (19.31a)$$

$$\boxed{\kappa = 19.1\left(\frac{k_Bc}{\sigma_T\ln\Lambda}\right)\left(\frac{k_BT_e}{m_ec^2}\right)^{5/2} = 4.4\times10^{-11}\left(\frac{T_e}{1\mathrm{K}}\right)^{5/2}\left(\frac{\ln\Lambda}{10}\right)^{-1}\ \mathrm{Wm}^{-1}\mathrm{K}^{-1}\ .} \quad (19.31b)$$

[5] For a detailed discussion, see, e.g., Binney & Tremaine (1987).

[6] Spitzer (1962).

Here σ_T is the Thomson cross section, Eq. (19.28). Note that neither transport coefficient depends explicitly upon the density; increasing the number of charge or heat carriers is compensated by the reduction in their mean free paths.

19.5.1 Anomalous Resistivity and Anomalous Equilibration

We have demonstrated that the theoretical Coulomb interaction between charged particles gives very long mean free paths and, consequently, very large electrical and thermal conductivities. Is this the way that real plasmas behave? The answer is invariably "no". As we shall show in the next three chapters, a plasma can support a variety of modes of "collective excitation" in which large numbers of electrons and/or ions move in collective, correlated fashions that are mediated by electromagnetic fields which they create. When the modes of a plasma are sufficiently strongly excited, the electromagnetic fields carried by the excitations can be much more effective than Coulomb scattering at deflecting the orbits of individual electrons and ions, and at feeding energy into or removing it from electrons and ions. Correspondingly, the electrical and thermal conductivities will be reduced. The reduced transport coefficients are termed *anomalous* and as we shall start to discuss in Chap. 21, it is one of the principal tasks of nonlinear plasma physics to provide quantitative calculations of these coefficients.

****

EXERCISES

Exercise 19.8 *Challenge: Thermoelectric Transport Coefficients*

(a) Consider a plasma in which the magnetic field is so weak that it presents little impediment to the flow of heat and electric current. Suppose that the plasma has a gradient $\boldsymbol{\nabla} T_e$ of its electron temperature and also has an electric field $\mathbf{E}$. It is a familiar fact that the temperature gradient will cause heat to flow and the electric field will create an electric current. Not so familiar, but somewhat obvious if one stops to think about it, is the fact that the temperature gradient also creates an electric current, and the electric field also causes heat flow. Explain in physical terms why this is so.

(b) So long as the mean free path of an electron between substantial deflections, $\ell_{\rm mfp} = (3k_B T_e/m_e)^{1/2} t_{D,e}$, is short compared to the lengthscale for substantial temperature change, $T_e/|\boldsymbol{\nabla} T_e|$, and short compared to the lengthscale for the electrons to be accelerated to near the speed of light by the electric field, $m_e c^2/eE$, the fluxes of heat $\mathbf{q}$ and of electric charge $\mathbf{J}$ will be governed by electron diffusion and will be linear in $\boldsymbol{\nabla} T$ and $\mathbf{E}$:

$$\mathbf{q} = -\kappa \boldsymbol{\nabla} T \ - \ \beta \mathbf{E} \ , \qquad \mathbf{J} = \kappa_e \mathbf{E} \ + \ \alpha \boldsymbol{\nabla} T \ . \tag{19.32}$$

The coefficients κ (heat conductivity), κ_e (electrical conductivity), β, and α are called *thermoelectric transport coefficients*. Use kinetic theory, in a situation where $\boldsymbol{\nabla} T =$

0, to derive the conductivity equations $\mathbf{J} = \kappa_e \mathbf{E}$ and $\mathbf{q} = -\beta \mathbf{E}$, and the following approximate formulae for the transport coefficients:

$$\kappa_e \sim \frac{ne^2 t_{D,e}}{m_e}, \qquad \beta \sim \frac{k_B T}{e} \kappa_e \ . \tag{19.33}$$

Show that, aside from a coefficient of order unity, this κ_e, when expressed in terms of the plasma's temperature and density, reduces to Eq. (19.31). The specific coefficients in Eq. (19.31) comes from a Fokker-Planck analysis.[7]

(c) Use kinetic theory, in a situation where $\mathbf{E} = 0$, to derive the conductivity equations $\mathbf{q} = -\kappa \boldsymbol{\nabla} T$ and $\mathbf{J} = \alpha \boldsymbol{\nabla} T$, and the approximate formulae

$$\kappa \sim k_B n \frac{k_B T_e}{m_e} t_{D,e} \ , \qquad \alpha \sim \frac{e}{k_B T_e} \kappa \ . \tag{19.34}$$

Show that, aside from a coefficient of order unity, this κ reduces to Eq. (19.31).[8]

(d) It can be shown[9] that for a hydrogen plasma it must be true that

$$\frac{\alpha \beta}{\kappa_e \kappa} = 0.581 \ . \tag{19.35}$$

By studying the entropy-governed probability distributions for fluctuations away from statistical equilibrium, one can derive another relation among the thermoelectric transport coefficients, the *Onsager relation*[10]

$$\beta = \alpha T + \frac{5}{2} \frac{k_B T_e}{e} \kappa_e \ ; \tag{19.36}$$

Equations (19.35) and (19.36) determine α and β in terms of κ_e and κ. Show that your approximate values of the transport coefficients, Eqs. (19.33) and (19.34), are in rough accord with Eqs. (19.35) and (19.36).

(e) If a temperature gradient persists for sufficiently long, it will give rise to sufficient charge separation in the plasma to build up an electric field (called a "secondary field") that prevents further charge flow. Show that this suppresses the heat flow: The total heat flux is then $\mathbf{q} = -\kappa_{T,\ \text{effective}} \boldsymbol{\nabla} T$, where

$$\kappa_{T,\ \text{effective}} = \left(1 - \frac{\alpha \beta}{\kappa_e \kappa}\right) \kappa = 0.419 \kappa \ . \tag{19.37}$$

****

[7] Spitzer (1962).
[8] *ibid*
[9] *ibid*
[10] Kittel (1958), Secs 33, 34; Reif (1965), Sec 15.8.

19.6 Magnetic Field

19.6.1 Cyclotron frequency and Larmor radius.

Many of the plasmas that we will encounter are endowed with a strong magnetic field. This causes the charged particles to travel along helical orbits about the field direction rather than move rectilinearly between collisions. If we designate the magnetic field strength $\mathbf{B}$, the equation of motion for an electron becomes

$$m_e \frac{d\mathbf{v}}{dt} = -e\mathbf{v} \times \mathbf{B} \, , \tag{19.38}$$

which gives rise to a constant speed $v_{||}$ parallel to the magnetic field and a circular motion perpendicular to the field with angular velocity

$$\boxed{\omega_c = \frac{eB}{m_e} = 1.76 \times 10^{11} \left(\frac{B}{1\,\mathrm{T}} \right) \ \ \mathrm{s}^{-1}.} \tag{19.39}$$

This angular velocity is called the *electron cyclotron frequency*, or simply the *cyclotron frequency*. Notice that this cyclotron frequency depends only on the magnetic field strength B and not on the plasma's density $\bar{n}$ or the electron velocity (i.e., the plasma temperature T). Neither does it depend upon the angle between $\mathbf{v}$ and $\mathbf{B}$, (called the *pitch angle*, α).

We also define a *Larmor radius*, r_L, which is the radius of the gyrational orbit projected perpendicular to the direction of the magnetic field. This is given by

$$\boxed{r_L = \frac{v_\perp}{\omega_c} = \frac{v \sin\alpha}{\omega_c} = 5.7 \times 10^{-7} \left(\frac{v_\perp}{1\mathrm{kms}^{-1}} \right) \left(\frac{B}{1\mathrm{T}} \right)^{-1} \ \mathrm{m} \, .} \tag{19.40}$$

Protons (and other ions) in a plasma also undergo cyclotron motion. Because their masses are larger by $m_p/m_e = 1836$ than the electron mass, their angular velocity

$$\boxed{\omega_{cp} = \frac{eB}{m_p} = 0.96 \times 10^8 \ \mathrm{s}^{-1} \left(\frac{B}{1\,\mathrm{T}} \right)} \tag{19.41}$$

is 1836 times lower. This quantity is called the *proton cyclotron frequency* or *ion cyclotron frequency*. The sense of gyration is, of course, opposite to that of the electrons. If the protons have similar temperatures to the electrons, their speeds are typically ~ 43 times smaller than those of the electrons, and their typical Larmor radii are ~ 43 times larger than those of the electrons.

We demonstrated above that all the electrons in a plasma can oscillate in phase at the plasma frequency. The electrons' cyclotron motion can also become coherent. Such coherent motions are called *cyclotron resonances* or *cyclotron oscillations*. Ion cyclotron resonances can also occur. Characteristic cyclotron frequencies and Larmor radii are tabulated in Table 19.1. It can be seen that the cyclotron frequency, like the plasma frequency, is typically larger than the the energy equilibration rates.

19.6.2 Validity of the Fluid Approximation.

In Chap. 17, we developed the magnetohydrodynamic (MHD) description of a magnetized plasma. We described the plasma by its density and temperature (or equivalently its pressure). Under what circumstances is this an accurate description? The answer to this question turns out to be quite complex and a full discussion would go well beyond this book. Some aspects are, however, easy to describe. One circumstance when a fluid description ought to be acceptable is when the timescales τ that characterize the macroscopic flow are long compared with time required to establish Maxwellian equilibrium (i.e. $\tau \gg \nu_{ei}^{-1}$), and the excitation level of collective wave modes is so small that these do not interfere seriously with the influence of Coulomb collisions. Unfortunately, this is rarely the case. (One type of plasma where this might be a quite good approximation is that in the interior of the sun.)

Magnetohydrodynamics can still provide a moderately accurate description of a plasma even if the electrons and ions are not fully equilibrated, when the electrical conductivity can be treated as very large and the thermal conductivity as very small. This means that we can treat the magnetic Reynolds' number as effectively infinite and the plasma and the equation of state as that of a perfect fluid (as we assumed in much of Chap. 17). It is not so essential that the actual particle distribution functions be Maxwellian, merely that they have second moments that can be associated with a common temperature. Quite often in plasma physics almost all of the dissipation is localized, for example to the vicinity of a shock front, and the remainder of the flow can be treated using MHD. The MHD description then provides a boundary condition for a fuller plasma physical analysis of the dissipative region. This simplifies the analysis of such situtations.

The great advantage of fluid descriptions, and the reason why physicists abandon them with such reluctance, is that they are much simpler than other descriptions of a plasma. One only has to cope with the pressure, density, and velocity and does not have to deal with an elaborate statistical description of the positions and velocities of all the particles. Generalizations of the simple fluid approximation have therefore been devised which can extend the domain of validity of simple MHD ideas. One extension, which we develop in the following chapter, is to treat the protons and the electrons as two separate fluids and derive dynamical equations to describe their (coupled) evolution. The other approach, which we describe now, is to acknowledge that, in most plasmas, the cyclotron period is very short compared with the Coulomb collision time and that the timescale on which energy is transferred backwards and forwards between the electrons and the protons and the electromagnetic field is intermediate between ω_c^{-1} and ν_{ee}^{-1}. Intuitively, this allows the electron and proton velocity distributions to become axisymmetric with respect to the magnetic field direction, though not fully isotropic. In other words, we can characterize the plasma using a density and two separate components of pressure, one associated with motion along the direction of the magnetic field, the other with gyration about the field.

For simplicity, let us just consider the electrons and their stress tensor, which we can write as

$$T_e^{jk} = \int \mathcal{N}_e p^j p^k \frac{d^3p}{m} \,, \tag{19.42}$$

where $\mathcal{N}_e$ is the electron number density in phase space; cf. Sec. 2.5. If we orient cartesian

axes so that the direction of $\mathbf{e}_z$ is parallel to the local magnetic field, then

$$\boxed{||T_e^{jk}|| = \begin{bmatrix} P_{e\perp} & 0 & 0 \\ 0 & P_{e\perp} & 0 \\ 0 & 0 & P_{e||} \end{bmatrix} ,} \tag{19.43}$$

where $P_{e\perp}$ is the electron pressure perpendicular to $\mathbf{B}$, and $P_{e||}$ is the electron pressure parallel to $\mathbf{B}$. Now suppose that there is a compression or expansion on a timescale that is long compared with the cyclotron period but short compared with the Coulomb collision timescale so that we should not expect that $P_{e\perp}$ is equal to $P_{e||}$ and we anticipate that they will evolve with density according to different laws.

The adiabatic indices governing $P_\perp$ and $P_{||}$ in such a situation are easily derived from kinetic theory arguments (Exercise 19.11): For compression *perpendicular* to $\mathbf{B}$ and no change of length along $\mathbf{B}$,

$$\boxed{\gamma_\perp \equiv \left(\frac{\partial \ln P_\perp}{\partial \ln \rho}\right)_s = 2 \ , \quad \gamma_{||} \equiv \left(\frac{\partial \ln P_{||}}{\partial \ln \rho}\right)_s = 1 \ .} \tag{19.44}$$

and for compression parallel to $\mathbf{B}$ and no change of transverse area,

$$\boxed{\gamma_\perp \equiv \left(\frac{\partial \ln P_\perp}{\partial \ln \rho}\right)_s = 1 \ , \quad \gamma_{||} \equiv \left(\frac{\partial \ln P_{||}}{\partial \ln \rho}\right)_s = 3 \ .} \tag{19.45}$$

By contrast if the expansion is sufficiently slow that Coulomb collisions are effective (though not so slow that heat conduction can operate), then we expect the velocity distribution to maintain isotropy and both components of pressure to evolve according to the law appropriate to a monatomic gas,

$$\boxed{\gamma = \left(\frac{\partial \ln P_\perp}{\partial \ln \rho}\right)_s = \left(\frac{\partial \ln P_{||}}{\partial \ln \rho}\right)_s = \frac{5}{3} \ .} \tag{19.46}$$

19.6.3 Conductivity Tensor

As is evident from the foregoing remarks, if we are in a regime where Coulomb scattering really does determine the particle mean free path, then an extremely small magnetic field strength suffices to ensure that individual particles complete gyrational orbits before they collide. Specifically, for electrons, the deflection time t_D, given by Eq. (19.20) exceeds ω_c^{-1} if

$$B \gtrsim 10^{-12} \left(\frac{n}{1\mathrm{cm}^{-3}}\right) \left(\frac{T_e}{1\mathrm{K}}\right)^{-3/2} \ \mathrm{T}. \tag{19.47}$$

This is almost always the case. It is also almost always true for the ions.

When inequality (19.47) is satisfied, the transport coefficients must be generalized to form tensors. Let us compute the electrical conductivity tensor for a plasma in which a steady electric field $\mathbf{E}$ is applied. Once again orienting our coordinate system so that the

magnetic field is parallel to $\mathbf{e}_z$, we can write down an equation of motion for the electrons by balancing the electromagnetic acceleration with the average rate of loss of momentum due to collisions.

$$-e(\mathbf{E}+\mathbf{v}\times\mathbf{B})-m_e\nu_D\mathbf{v}=0 \tag{19.48}$$

Solving for the velocity we obtain

$$\begin{pmatrix} v_x \\ v_y \\ v_z \end{pmatrix} = -\frac{e}{m_e\nu_D(1+\omega_c^2/\nu_D^2)} \begin{pmatrix} 1 & \omega_c/\nu_D & 0 \\ -\omega_c/\nu_D & 1 & 0 \\ 0 & 0 & 1+\omega_c^2/\nu_D^2 \end{pmatrix} \begin{pmatrix} E_x \\ E_y \\ E_z \end{pmatrix} . \tag{19.49}$$

As the current density is $\mathbf{j}_e=-n\mathbf{v}=\kappa_e\mathbf{E}$, the electrical conductivity tensor is given by

$$\boxed{\kappa_e = \frac{ne^2}{m_e\nu_D(1+\omega_c^2/\nu_D^2)} \begin{pmatrix} 1 & \omega_c/\nu_D & 0 \\ -\omega_c/\nu_D & 1 & 0 \\ 0 & 0 & 1+\omega_c^2/\nu_D^2 \end{pmatrix} .} \tag{19.50}$$

It is apparent from the form of this conductivity tensor that when $\omega_c \gg \nu_D$, the conductivity perpendicular to the magnetic field is greatly inhibited, whereas that along the magnetic field is unaffected. Similar remarks apply to the flow of heat. It is therefore often assumed that only transport parallel to the field is effective. However, as is made clear in the next section, if the plasma is inhomogeneous, cross-field transport can be quite rapid in practice.

****

EXERCISES

Exercise 19.9 *Example: Relativistic Larmor radius*
Use the relativistic equation of motion to show that the relativistic electron cyclotron frequency is $\omega_c = eB/\gamma m_e$where γ is the electron Lorentz factor. What is the relativistic Larmor radius?

Exercise 19.10 *Example: Ultra-High-Energy Cosmic Rays*
The most energetic cosmic ray reported in recent years is believed to be a proton and to have an energy $\sim 3\times10^{20}$ eV. In order to arrive at earth, it must have passed through a perpendicular Galactic magnetic field of strength 0.3 nT for a distance of ~ 1000 light year. Through what angle will it have been deflected?

Exercise 19.11 *Problem: Adiabatic Indices for Rapid Compression of a Magnetized Plasma*
Consider a plasma in which, in the local rest frame of the electrons, the electron stress tensor has the form (19.43) with $\mathbf{e}_z \equiv \mathbf{b}$ the direction of the magnetic field. The following analysis for the electrons can be carried out independently for the ions, with the same resulting formulae.

(a) Show that

$$P_{e||} = nm_e\langle v_{||}^2\rangle \ , \quad P_{e\perp} = \frac{1}{2}nm_e\langle|\mathbf{v}_\perp|^2\rangle \ , \tag{19.51}$$

where $\langle v_{||}^2 \rangle$ is the mean square electron velocity parallel to $\mathbf{B}$ and $\langle |\mathbf{v}_\perp|^2 \rangle$ is the mean square velocity orthogonal to $\mathbf{B}$. (The velocity distributions are *not* assumed to be Maxwellian.)

(b) Consider a fluid element with length l along the magnetic field and cross sectional area A orthogonal to the field. Let $\bar{\mathbf{v}}$ be the mean velocity of the electrons ($\bar{\mathbf{v}} = 0$ in the mean electron rest frame) and let θ and σ_{jk} be the expansion and shear of the mean electron motion as computed from $\bar{\mathbf{v}}$. Show that

$$\frac{dl/dt}{l} = \frac{1}{3}\theta + \sigma^{jk} b_j b_k \ , \quad \frac{dA/dt}{A} = \frac{2}{3}\theta - \sigma^{jk} b_j b_k \ , \tag{19.52}$$

where $\mathbf{b} = \mathbf{B}/|\mathbf{B}| = \mathbf{e}_z$ is a unit vector in the direction of the magnetic field.

(c) Assume that the timescales for compression and shearing are short compared to the Coulomb-scattering electron-deflection timescale, $\tau \ll t_{D,e}$. Show, using the laws of energy and particle conservation, that

$$\begin{aligned} \frac{1}{\langle v_{||}^2 \rangle} \frac{d\langle v_{||}^2 \rangle}{dt} &= -\frac{2}{l}\frac{dl}{dt} \ , \\ \frac{1}{\langle v_\perp^2 \rangle} \frac{d\langle v_\perp^2 \rangle}{dt} &= -\frac{1}{A}\frac{dA}{dt} \ , \\ \frac{1}{n}\frac{dn}{dt} &= -\frac{1}{l}\frac{dl}{dt} - \frac{1}{A}\frac{dA}{dt} \ . \end{aligned} \tag{19.53}$$

(d) Show that

$$\begin{aligned} \frac{1}{P_{e||}} \frac{dP_{e||}}{dt} &= -3\frac{dl/dt}{l} - \frac{dA/dt}{A} = -\frac{5}{3}\theta - 2\sigma^{jk} b_j b_k \ , \\ \frac{1}{P_{e\perp}} \frac{dP_{e\perp}}{dt} &= -\frac{dl/dt}{l} - 2\frac{dA/dt}{A} = -\frac{5}{3}\theta + \sigma^{jk} b_j b_k \ . \end{aligned} \tag{19.54}$$

(e) Show that when the fluid is expanding or compressing entirely perpendicular to $\mathbf{B}$, with no expansion or compression along $\mathbf{B}$, the pressures change in accord with the adiabatic indices of Eq. (19.44). Show, similarly, that when the fluid expands or compresses along $\mathbf{B}$, with no expansion or compression in the perpendicular direction, the pressures change in accord with the adiabatic indices of Eq. (19.45).

(f) Hence derive the so-called *double adiabatic* equations of state

$$P_\perp^2 P_\parallel \propto n^5 \ , \quad P_\perp \propto nB \ , \tag{19.55}$$

valid for changes on timescales long compared with the cyclotron period but short compared with all Coulomb collision times. [11]

****

[11] See Chew, Goldberger & Low (1956)

19.7 Adiabatic Invariants

In the next three chapters we shall meet a variety of plasma phenomena that can be understood in terms of the orbital motions of individual electrons and ions. These phenomena typically entail motions in an electromagnetic field that is nearly, but not quite spatially homogeneous on the scale of the Larmor radius r_L, and that is nearly but not quite constant during a cyclotron period $2\pi/\omega_c$. In this section, in preparation for the next three chapters, we shall review charged particle motion in such nearly homogeneous, nearly time-independent fields.

Since the motions of electrons are usually of greater interest than those of ions, we shall presume throughout this section that the charged particle is an electron; and we shall denote its charge by $-e$ and its mass by m_e.

19.7.1 Homogeneous, time-independent magnetic field

From the nonrelativistic version of the Lorentz force equation, $d\mathbf{v}/dt = -(e/m_e)\mathbf{v}\times\mathbf{B}$, one readily deduces that an electron in a homogeneous, time-independent magnetic field $\mathbf{B}$ moves with uniform velocity $\mathbf{v}_{||}$ parallel to the field, and moves perpendicular to the field in a circular orbit with the cyclotron frequency $\omega_c = eB/m_e$ and Larmor radius $r_L = m_e v_\perp/eB$. Here $v_\perp$ is the electron's time-independent transverse speed (speed perpendicular to $\mathbf{B}$).

19.7.2 Homogeneous time-independent electric and magnetic fields

Suppose that the homogeneous magnetic field $\mathbf{B}$ is augmented by a homogeneous electric field $\mathbf{E}$; and assume, initially, that $|\mathbf{E}\times\mathbf{B}| < B^2 c$. Then examine the electric and magnetic fields in a new reference frame, one that moves with the velocity

$$\boxed{\mathbf{v}_D = \frac{\mathbf{E}\times\mathbf{B}}{B^2}} \tag{19.56}$$

relative to the original frame. Note that the moving frame's velocity $\mathbf{v}_D$ is perpendicular to both the magnetic field and the electric field. From the Lorentz transformation law for the electric field, $\mathbf{E}' = \gamma(\mathbf{E} + \mathbf{v}_D\times\mathbf{B})$, we infer that in the moving frame the electric field and the magnetic field are parallel to each other. As a result, in the moving frame the electron's motion perpendicular to the magnetic field is purely circular; and, correspondingly, in the original frame its perpendicular motion consists of a *drift* with velocity $\mathbf{v}_D$, and superimposed on that drift, a circular motion (Fig. 19.4). In other words, the electron moves in a circle whose center (the electron's *guiding center*) drifts with velocity $\mathbf{v}_D$. Notice that the drift velocity (19.56) is independent of the electron's charge and mass, and thus is the same for ions as for electrons. This drift is called *the* $\mathbf{E}\times\mathbf{B}$ *drift*.

When the component of the electric field orthogonal to $\mathbf{B}$ is so large that the drift velocity computed from (19.56) exceeds the speed of light, the electron's guiding center, of course, cannot move with that velocity. Instead, the electric field drives the electron up to higher and higher velocities as time passes, but in a sinusoidally modulated manner. Ultimately the electron velocity gets arbitrarily close to the speed of light.

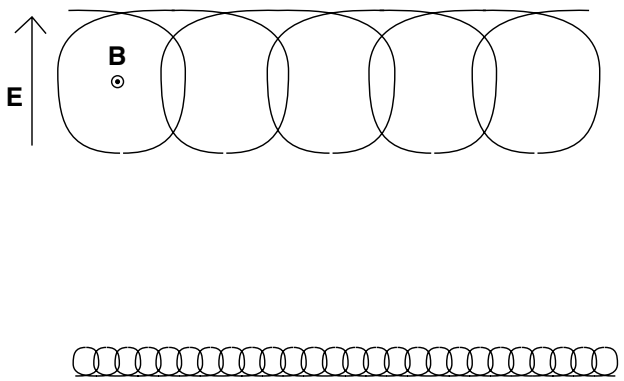

Fig. 19.4: The electron motion (upper diagram) and proton motion (lower diagram) orthogonal to the magnetic field, when there are constant electric and magnetic fields with $|\mathbf{E}\times\mathbf{B}| < B^2c$. Each electron and proton moves in a circle with a superposed drift velocity $\mathbf{v}_D$ given by Eq. (19.56).

When a uniform, time-independent gravitational field $\mathbf{g}$ accompanies a uniform, time-independent magnetic field $\mathbf{B}$, its effect on an electron will be the same as that of an electric field $\mathbf{E}_{\rm equivalent} = -(m_e/e)\mathbf{g}$: The electron's guiding center will acquire a drift velocity

$$\mathbf{v}_D = -\frac{m_e}{e}\frac{\mathbf{g}\times\mathbf{B}}{B^2}\ , \tag{19.57}$$

and similarly for a proton. This *gravitational drift* velocity is typically very small.

19.7.3 Inhomogeneous, time-independent magnetic field

When the electric field vanishes, the magnetic field is spatially *inhomogeneous* and time-independent, and the inhomogeneity scale is large compared to the Larmor radius r_L of the electron's orbit, the electron motion is nicely described in terms of a guiding center.

Consider, first, the effects of a curvature of the field lines (Fig. 19.5a). Suppose that the speed of the electron along the field lines is $v_{||}$. We can think of this as a guiding center motion. As the field lines bend in, say, the direction of the unit vector $\mathbf{n}$ with radius of curvature R, this longitudinal guiding-center motion experiences the acceleration $\mathbf{a} = v_{||}^2\mathbf{n}/R$. That acceleration is equivalent to the effect of an electric field $\mathbf{E}_{\rm effective} = (-m_e/e)v_{||}^2\mathbf{n}/R$, and it therefore produces a drift of the guiding center with $\mathbf{v}_D = (\mathbf{E}_{\rm effective}\times\mathbf{B})/B^2$. Since the curvature R of the field line and the direction $\mathbf{n}$ of its bend are given by $B^{-2}(\mathbf{B}\cdot\boldsymbol{\nabla})\mathbf{B} = \mathbf{n}/R$, this *curvature drift* velocity is

$$\boxed{\mathbf{v}_D = \frac{m_e v_{||}^2 c}{e}\mathbf{B}\times\frac{(\mathbf{B}\cdot\boldsymbol{\nabla})\mathbf{B}}{B^4}\ .} \tag{19.58}$$

Notice that the magnitude of this drift is

$$v_D = \frac{r_L}{R}\frac{v_{||}}{v_\perp}v_{||}\ . \tag{19.59}$$

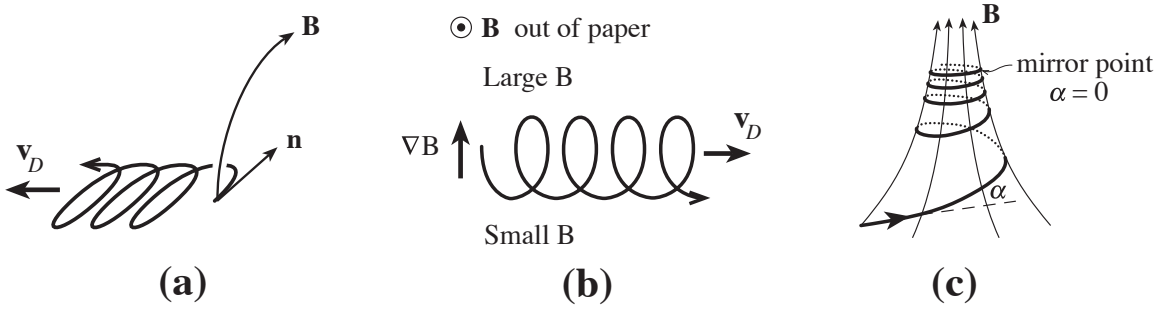

Fig. 19.5: An electron's motion in a time-independent, inhomogeneous magnetic field. (a) The drift induced by the curvature of the field lines. (b) The drift induced by a transverse gradient of the magnitude of the magnetic field. (c) The change in electron pitch angle induced by a longitudinal gradient of the magnitude of the magnetic field.

A second kind of inhomogeneity is a transverse spatial gradient of the magnitude of $\mathbf{B}$. As is shown in Fig. 19.5b, such a gradient causes the electron's circular motion to be tighter (smaller radius of curvature of the circle) in the region of larger B than in the region of smaller B; and this difference in radii of curvature clearly induces a drift. It is straightforward to show that the resulting *gradient drift* velocity is

$$\boxed{\mathbf{v}_D = \frac{-m_e v_\perp^2 c}{2e} \frac{\mathbf{B} \times \boldsymbol{\nabla} B}{B^3} \ .} \tag{19.60}$$

A third, and last, kind of inhomogeneity is a longitudinal gradient of the magnitude of $\mathbf{B}$ Fig. 19.5c. Such a gradient results from the magnetic field lines converging toward each other (or diverging away from each other). The effect of this convergence is most easily inferred in a frame that moves longitudinally with the electron. In such a frame the magnetic field changes with time, $\partial \mathbf{B}'/\partial t \neq 0$, and correspondingly there is an electric field that satisfies $\boldsymbol{\nabla} \times \mathbf{E}' = -\partial \mathbf{B}'/\partial t$. The kinetic energy of the electron as measured in this longitudinally moving frame is the same as the transverse energy $\frac{1}{2} m_e v_\perp^2$ in the original frame. This kinetic energy is forced to change by the electric field $\mathbf{E}'$. The change in energy during one circuit around the magnetic field is

$$\Delta \left(\frac{1}{2} m_e v_\perp^2 \right) = -e \oint \mathbf{E}' \cdot d\mathbf{l} = e \int \frac{\partial \mathbf{B}'}{\partial t} \cdot d\mathbf{A} = e \left(\frac{\omega_c}{2\pi} \Delta B \right) \pi r_L^2 = \frac{m_e v_\perp^2}{2} \frac{\Delta B}{B} \ . \tag{19.61}$$

Here the second expression involves a line integral once around the electron's circular orbit and has $\partial \mathbf{B}'/\partial t$ parallel to $d\mathbf{A}$; the third expression involves a surface integral over the interior of the orbit; in the fourth the time derivative of the magnetic field has been expressed as $(\omega_c/2\pi)\Delta B$ where ΔB is the change in magnetic field strength along the electron's guiding center during one circular orbit.

Equation (19.61) can be rewritten as a conservation law along the world line of the electron's guiding center:

$$\frac{m_e v_\perp^2}{2B} = \text{constant} \ . \tag{19.62}$$

Notice that the conserved quantity $m_e v_\perp^2/2B$ is equal to $1/2\pi$ times the total magnetic flux threading through the electron's circular orbit, $\pi r_L^2 B$; thus, *the electron moves along the field lines in such a manner as to keep the magnetic flux enclosed within its orbit always constant*; see Fig. 19.5c. A second interpretation of (19.62) is in terms of the magnetic moment created by the electron's circulatory motion; that moment is $\boldsymbol{\mu} = (-m_e v_\perp^2/2B^2)\mathbf{B}$; and its magnitude is the conserved quantity

$$\boxed{\mu = \frac{m_e v_\perp^2}{2B} = \text{constant}\ .} \tag{19.63}$$

An important consequence of the conservation law (19.62) is a gradual change in the electron's *pitch angle*

$$\alpha \equiv \tan^{-1}(v_{||}/v_\perp) \tag{19.64}$$

as it spirals along the converging field lines: Because there is no electric field in the original frame, the electron's total kinetic energy is conserved in that frame,

$$E_{\rm kin} = m_e \frac{1}{2}(v_{||}^2 \ + \ v_\perp^2) = \text{constant}\ . \tag{19.65}$$

This, together with the constancy of $\mu = m_e v_\perp^2/2B$ and the definition (19.64) of the electron pitch angle, implies that the pitch angle varies with magnetic field strength as

$$\boxed{\tan^2\alpha = \frac{E_{\rm kin}}{\mu B} - 1\ .} \tag{19.66}$$

Notice that as the field lines converge, B increases in magnitude, and α decreases. Ultimately, when B reaches a critical value $B_{\rm crit} = E_{\rm kin}/\mu$, the pitch angle α goes to zero. The electron then "reflects" off the strong-field region and starts moving back toward weak fields, with increasing pitch angle. The location at which the electron reflects is called the electron's *mirror point*.

Figure 19.6 shows two examples of this mirroring. The first example is a "magnetic bottle." Electrons whose pitch angles at the center of the bottle are sufficiently small have mirror points within the bottle and thus cannot leak out. The second example is the van Allen belts of the earth. Electrons (and also ions) travel up and down the magnetic field lines of the van Allen belts, reflecting at mirror points.

It is not hard to show that the gradient of $\mathbf{B}$ can be split up into the three pieces we have studied: a curvature with no change of $B = |\mathbf{B}|$ (Fig. 19.5a), a change of B orthogonal to the magnetic field (Fig. 19.5b), and a change of B along the magnetic field (Fig. 19.5c). When (as we have assumed) the lengthscales of these changes are far greater than the electron's Larmor radius, their effects on the electron's motion superpose linearly.

19.7.4 A slowly time varying magnetic field

When the magnetic field changes on timescales long compared to the cyclotron period $2\pi/\omega_c$, its changes induce alterations of the electron's orbit that can be deduced with the aid of

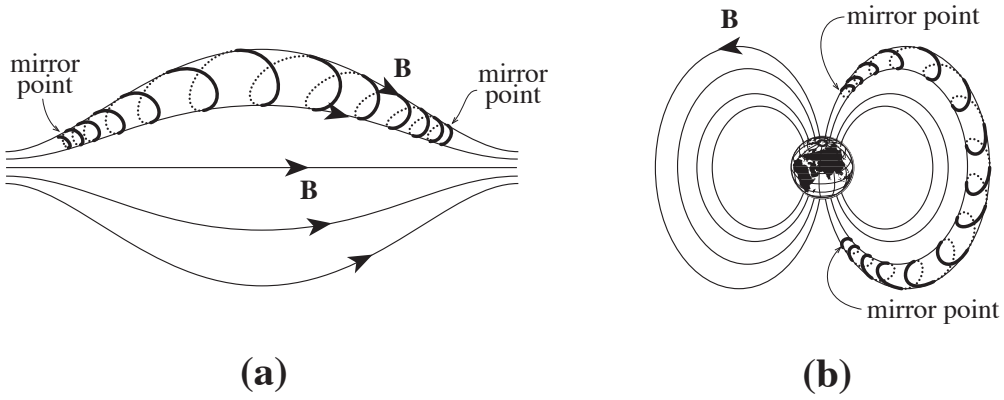

Fig. 19.6: Two examples of the mirroring of particles in an inhomogeneous magnetic field: (a) A magnetic bottle. (b) The earth's van Allen belts.

adiabatic invariants—i.e., quantities that are invariant when the field changes adiabatically (slowly).[12]

The conserved magnetic moment $\mu = m_e v_\perp^2/2B$ associated with an electron's transverse, circular motion is an example of an adiabatic invariant. We proved its invariance in Eqs. (19.61) and (19.62) above (where we were computing in a reference frame in which the magnetic field changed slowly, and associated with that change there was a weak electric field). This adiabatic invariant can be shown to be, aside from a constant multiplicative factor $2\pi m_e c/e$, the action associated with the electron's circular motion, $J_\phi = \oint p_\phi d\phi$. Here ϕ is the angle around the circular orbit and $p_\phi = m_e v_\perp r_L - eA_\phi$ is the ϕ component of the electron's canonical momentum. The action J_ϕ is a well-known adiabatic invariant.

Whenever a slightly inhomogeneous magnetic field varies slowly in time, not only is $\mu = m_e v_\perp^2/2B$ adiabatically invariant (conserved); so also are two other actions. One is the action associated with motion from one mirror point of the magnetic field to another and back,

$$J_{||} = \oint \mathbf{p}_{||} \cdot d\,\mathbf{l}\,. \tag{19.67}$$

Here $\mathbf{p}_{||} = m_e \mathbf{v}_{||} - e\mathbf{A}_{||} = m_e \mathbf{v}_{||}$ is the generalized (canonical) momentum along the field line, and $d\,\mathbf{l}$ is distance along the field line; so the adiabatic invariant is the spatial average $\langle v_{||} \rangle$ of the longitudinal speed of the electron, multiplied by twice the distance Δl between mirror points, $J_{||} = 2\langle v_{||} \rangle \Delta l$.

The other (third) adiabatic invariant is the action associated with the drift of the guiding center: an electron mirroring back and forth along the field lines drifts sideways, and by its drift it traces out a 2-dimensional surface to which the magnetic field is parallel—e.g., the surface of the magnetic bottle in Fig. 19.6a. The action of the electon's drift around this magnetic surface turns out to be proportional to the total magnetic flux enclosed within the surface. Thus, if the field geometry changes very slowly, the magnetic flux enclosed by the magnetic surface on which the electron moves is adiabatically conserved.

[12]See e.g. Landau & Lifshitz (1960), Northrop (1963).

How nearly constant are the adiabatic invariants? The general theory of adiabatic invariants shows that, so long as the temporal changes of the magnetic field structure are smooth enough to be described by analytic functions of time, then the fractional failures of the adiabatic invariants to be conserved are of order $e^{-\tau/P}$, where τ is the timescale on which the field changes and P is the period of the motion associated with the adiabatic invariant ($2\pi/\omega_c$ for the invariant μ; the mirroring period for the longitudinal action; the drift period for the magnetic flux enclosed in the electron's magnetic surface). Because the exponential $e^{-\tau/P}$ dies out so quickly with increasing timescale τ, the adiabatic invariants are conserved to very high accuracy whenever $\tau \gg P$.

****

EXERCISES

Exercise 19.12 *Example: Mirror Machine*
One method for confining hot plasma is to arrange electric coils so as to make a mirror machine in which the magnetic field has the geometry sketched in Fig. 19.6a. Suppose that the magnetic field in the center is 1 T and the field strength at the two necks is 10 T, and that plasma is introduced with an isotropic velocity distribution near the center of the bottle.

(a) What fraction of the plasma particles will escape?

(b) Sketch the pitch angle distribution function for the particles that remain.

(c) Suppose that Coulomb collisions cause particles to diffuse in pitch angle α with a diffusion coefficient

$$D_{\alpha\alpha} \equiv \left\langle \frac{\Delta\alpha^2}{\Delta t} \right\rangle = t_D^{-1} \tag{19.68}$$

Estimate how long it will take most of the plasma to escape the mirror machine.

(d) What do you suspect will happen in practice?

Exercise 19.13 *Challenge: Penning Traps*
A clever technique for studying the behavior of individual electrons or ions is to entrap them using a combination of electric and magnetic fields. One of the simplest and most useful devices is the *Penning trap.*[13] Basically this comprises a uniform magnetic field B combined with a hyperboloidal electrostatic field that is maintained between hyperboloidal electrodes as shown in Fig. 19.7. The electrostatic potential has the form $\Phi(\mathbf{x}) = \Phi_0(z^2 - x^2/2 - y^2/2)/2d^2$, where Φ_0 is the potential difference maintained across the electrodes, d is the minimum axial distance from the origin to the hyperloidal cap as well as $1/\sqrt{2}$ times the minimum radius of the ring electrode.

(a) Show that the potential satisfies Laplace's equation, as it must.

[13] Brown & Gabrielse (1986)

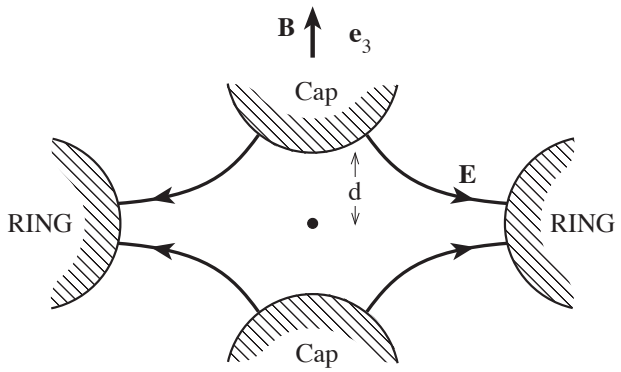

Fig. 19.7: Penning Trap for localizing individual charged particles. The magnetic field is uniform and parallel to the axis of symmetry $\mathbf{e}_3$. The electric field is maintained between a pair of hyperboloidal caps and a hyperboloidal ring.

(b) Now consider an individual charged particle in the trap. Show that there can be three separate oscillations excited:

(i) Cyclotron orbits in the magnetic field with angular frequency ω_c,

(ii) "Magnetron" orbits produced by $\mathbf{E} \times \mathbf{B}$ drift around the axis of symmetry with angular frequency ω_m,

(iii) Axial oscillations parallel to the magnetic field with angular frequency ω_z.

Assume that $\omega_m \ll \omega_z \ll \omega_c$ and show that $\omega_z^2 \simeq 2\omega_m\omega_c$.

(c) Typically the potential difference across the electrodes is ~ 10 V, the magnetic field strength is $B \sim 6$ T, and the radius of the ring and the height of the caps above the center of the traps are ~ 3 mm. Estimate the three independent angular frequencies for electrons and ions verifying the ordering $\omega_m \ll \omega_z \ll \omega_c$. Also estimate the maximum velocities associated with each of these oscillations if the particle is to be retained by the trap.

(d) Solve the classical equation of motion exactly and demonstrate that the magnetron motion is formally unstable.

Penning traps have been used to perform measurements of the electron-proton mass ratio and the magnetic moment of the electron with unprecedented precision.

****

Bibliographic Note

For a very thorough treatment of the particle kinetics of plasmas, see Shkarofsky, Johnston and Bachynski (1966). For less detailed treatments see the relevant portions of Boyd and

Box 19.2
Important Concepts in Chapter 18

- Density-Temperature regime for plasmas, Sec. 19.2 and Fig. 19.1
- Examples of environments where plasmas occur, Sec. 19.2, Fig. 19.1, and Table 19.1
- Debye shielding, Debye length and Debye number, Secs. 19.3.1 and 19.3.2
- Plasma oscillations and plasma frequency, Sec. 19.3.3
- Coulomb logarithm, its role in quantifying the cumulative effects of small-angle Coulomb scatterings, and its typical values, Secs. 19.4.1, 19.4.2
- Deflection times t_D and rates ν_D for Coulomb collisions (ee, pp and ep), Sec. 19.4.1
- Thermal equilibration times t_E and rates $\nu_E = 1/t_E$ for Coulomb collisions (ee, pp, and ep and their ratios), Sec. 19.4.3
- Electric and thermal conductivity for an unmagnetized plasma when the principal impediment is Coulomb scattering, Sec. 19.5
- Anomalous resistivity and equilibration, Sec. 19.5
- Cyclotron frequency for electrons and protons; Larmor radius, Sec. 19.6.1
- Anisotropic pressures, adiabatic indices, and electrical conductivity in a magnetized plasma, Secs. 19.6.2 and 19.6.3
- Drift velocities: $\mathbf{E} \times \mathbf{B}$ drift, curvature drift, and gradient drift, Secs. 19.7.2, and 19.7.3
- Adiabatic invariants for charged particle motion in an inhomogenous, time-varying magnetic field, and the character of the particle motion, Secs. 19.7.3, 19.7.4, and Fig. 19.6

Sanderson (1969), Krall and Trivelpiece (1973), Jackson (1999), Schmidt (1979), and especially Spitzer (1962). For particle motion in inhomogeneous and time varying magnetic fields, see Northrop (1963) and the relevant portions of Jackson (1999).

Bibliography

Binney, J.J. and Tremaine, S.D. 1987. *Galactic Dynamics*, Princeton, NJ: Princeton University Press.

Boyd, T.J.M. and Sanderson, J.J. 1969. *Plasma Dynamics*, London: Nelson.

Brown, L.S. and Gabrielse, G. 1986. "Geonium theory: Physics of a single electron or ion in a Penning trap." *Reviews of Modern Physics*, **58**, 233.

Chew, C.F., Goldberger, M.L. and Low, F.E. 1956. *Proceedings of the Royal Society of London*, **A236**, 112.

Crookes, W. (1879). *Phil. Trans.*, **1**, 135.

Heaviside, O. 1902. ????

Jackson, J.D. 1999. *Classical Electrodynamics*, third edition. New York: Wiley.

Kittel, C. 1958. *Elementary Statistical Physics*. New York: Wiley.

Krall, N.A. and Trivelpiece, A.W. 1973. *Principles of Plasma Physics*. New York: McGraw Hill.

Landau, L.D. and Lifshitz, E.M. 1960. *Mechanics*. Oxford: Pergamon Press.

Leighton, R.B. 1959. *Principles of Modern Physics*. New York: McGraw Hill.

Northrop, T.G. 1963. *Adiabatic Motion of Charged Particles*. New York: Interscience.

Reif, F. 1965. *Fundamentals of Statistical and Thermal Physics*. New York: McGraw Hill.

Rosenbluth, M.N., Macdonald, M., and Judd, D.L. 1957. *Physical Review*, ???.

Schmidt, G. 1979. *Physics of High Temperature Plasmas*. New York: Academic Press.

Shkarofsky, I.P., Johnston, T.W., and Bachynski, M.P. 1966. *The Particle Kinetics of Plasmas*, Reading Mass.: Addison-Wesley.

Spitzer, Jr., L. 1962. *Physics of Fully Ionized Gases*, second edition. New York: Interscience.